Nuclear Materials and Energy 42 (2025) 101903

Contents lists available at ScienceDirect

Nuclear Materials and Energy

journal homepage: www.elsevier.com/locate/nme

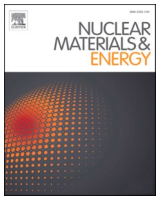

Experiment-modeling studies comparing energy dissipation in the DIII-D SAS and SAS-VW divertors☆,☆

D.M. Thomas [a], T. Abrams [a], R. Ding [b], D. Donovan [c], F. Effenberg [d], J. Herfindal [e], A. Hyatt [a], A.W. Leonard [a], X. Ma [a], R. Maurizio [a], A.G. McLean [f], C. Murphy [a], J. Ren [c], M.W. Shafer [e], D. Truong [g], H.Q. Wang [a], J.G. Watkins [g], J.H. Yu [a]

[a] General Atomics, General Atomics, San Diego, CA, USA
[b] ASIPP, Hefei, China
[c] University of Tennessee, Knoxville, TN, USA
[d] Princeton Plasma Physics Laboratory, Princeton, NJ, USA
[e] Oak Ridge National Laboratory, Oak Ridge, TN, USA
[f] Lawrence Livermore National Laboratory, Livermore, CA, USA
[g] Sandia National Laboratory, Albuquerque, NM, USA

ARTICLE INFO

Keywords:
Divertor
Dissipation
Detachment
Drifts
Closure
Modeling

ABSTRACT

Recent DIII-D experiments on Small Angle Slot (SAS) divertors have confirmed that a combination of divertor closure and target shaping can enhance cooling across the divertor target and increase energy dissipation, but with significant dependence on B_T (toroidal magnetic field) direction. In these novel divertors, the roles of closure, target shaping, drifts, and scale lengths are all interconnected in optimizing dissipation, with the separatrix electron density n_{eSEP} being the key parameter associated with the level of dissipation/detachment. After modifying the original flat-targeted graphite SAS to include a V shape with a tungsten coating on the outer side of the divertor (SAS-VW), matched series of discharges were run to compare to detailed SOLPS-ITER modeling. Experimentally, when run as designed with the outer strike point at the slot vertex, SAS-VW requires nearly identical n_{eSEP} for detachment as the original SAS, with little difference in dissipation for the new geometry. This is in contrast to (1) earlier modeling predictions that a small change of the SAS geometry to a V shape should enhance dissipation at the same n_{eSEP} for magnetic configurations having better H-mode access (ion $B \times \nabla B$ drift directed into the divertor), and (2) despite the achievement of significantly higher (2-7x) neutral pressures and compression in the SAS-VW slot. Comparisons of experimental density scans to the most recent SOLPS-ITER modeling with ExB drifts show reasonable agreement for dissipation/detachment onset when using separatrix density as the independent parameter. In order to help understand the discrepancy in modeled vs actual performance for the new configuration, additional measurements varying gas injection location and impurity injection were undertaken. In-slot D_2 gas fueling is more effective (5–22 %) in promoting detachment, in accord with modeling. In-slot impurity injection (N_2 or Ne) can yield 30 % lower core Z_{eff} and 15 % less confinement degradation after detachment compared to main chamber puffing, as well as relatively lower tungsten leakage from the divertor. Modeling can also reproduce the improved detachment seen as the strike point moves inboard of the slot vertex.

While we can explain the effects of the most important parameters causing energy dissipation in these slot divertors, it remains that many aspects of their behavior cannot be accurately modeled using state-of-art codes such as SOLPS-ITER. This is of concern for future model-driven designs utilizing similar V-shaped geometries.

☆ Supported by US DOE under DE-FC02-04ER54698, DE-SC0020093, DE-SC0019256, DE-AC02-09CH11466, DE-AC05-00OR22725, DE-AC52-07NA27344, and DE-NA0003525.☆ This article is part of a special issue entitled: 'PSI-26' published in Nuclear Materials and Energy.

E-mail address: thomas@fusion.gat.com (D.M. Thomas).

https://doi.org/10.1016/j.nme.2025.101903
Received 13 June 2024; Received in revised form 2 January 2025; Accepted 12 February 2025
Available online 13 February 2025

Introduction

Two key remaining issues for the development of steady-state fusion devices are the design of highly dissipative divertors and appropriate plasma facing materials. This is due to inherent limitations on divertor target heat load ($q_\perp \leq$ 10–15 MW m^{-2}), and plasma temperature at the divertor target plate ($Te \leq$ 5–10 eV to suppress physical erosion) [1,2]. Efficient divertor designs rely on a number of tools, viz. closure (for efficient retention of the recycled particle flux for dissipation), target shaping (for directing the recycled flux profile to high heat flux regions), *Te* gradient-generated E × B flows [3] (again, optimizing the particle flow to regions of higher heat flux), and injection of non-hydrogenic impurities (which enhance dissipation by increasing radiative losses). The inclusion of E × B drift flows in a closed geometry has two important effects: the natural (open) flow patterns can be frustrated or damped by small-scale physical structures, and the resulting altered flow patterns can enhance or diminish the localized recycling fluxes.

Recent improvements in drift-dependent modeling of the coupled edge plasma-neutral region using the SOLPS-ITER code [4,5,6] allow for efficient modeling of sophisticated divertor geometries and fueling strategies prior to an actual construction; however, it is crucial that these codes be validated against specific experimental configurations. Investigating these tools and techniques is critical to assess their feasibility, effectiveness, and scalability to a Fusion Pilot Plant (FPP).

This paper covers such a coupled experiment-modeling comparison using two different closed divertor geometries on DIII-D. The remainder of the paper is organized as follows: in the next section we describe a brief history and description of the divertor design, installation, and operation on DIII-D along with the progression of associated modeling using the SOLPS-ITER simulations of increasing sophistication. In the subsequent two sections we cover the results of energy dissipation studies on the divertors and point out areas of both agreement and disagreement with the modeling results. Finally, we conclude with a discussion of the results and some possible areas for improvement of future studies.

Experimental setup and modeling

Previous work with SAS

On DIII-D, the original small-angle slot (SAS) divertor [7] was constructed based on (drift-free) SOLPS-ITER modeling [8,9] which indicated the combination of divertor closure with appropriate target shaping could be used to enhance neutral cooling across the divertor target and increase dissipation compared to a more open divertor. SAS was able to demonstrate enhanced dissipation with detachment at lower line-averaged densities, consistent with the initial modeling results. However, a large asymmetry in detachment behavior was observed with respect to toroidal magnetic field direction, where for the ion b × ∇B drift into the divertor (the direction favorable to H-mode access) there was little benefit for detachment behavior with the slot compared to an open divertor configuration [10]. The asymmetric behavior of these results can be understood in terms of **E** × **B** drifts interacting with the localized recycling in the SAS. Coincident with these initial experimental results were advances in the drift implementation in the code, such that additional modeling with drifts turned on in SOLPS-ITER indicated the poloidal/radial **E** × **B** particle drifts within the slot could essentially explain the difference in the SAS detachment behavior [11].

SAS VW design and experiment

Subsequently, further design modeling using SOLPS-ITER indicated that a small change of the inner slot surface to a V-shape (SAS-V) should mitigate the observed drift-dependent asymmetry in dissipation for opposite toroidal field directions i.e., for the case of ion $\boldsymbol{B} \times \nabla B$ drift into the divertor the dissipation efficiency for a given upstream density should be improved [12,13]. The simulations for both the SAS and SAS-VW models were run in a similar fashion and included all charged states of deuterium and carbon. Details of the SAS-VW discharge modeling setup are described more fully in section 2 of Ref 12. Neutrals are modeled kinetically using the EIRENE solver. All simulations are conducted in a steady state and correspond to the inter-ELM phase of experiments. A fixed upstream separatrix density is used as a boundary constraint on each simulation to achieve a modeled density ramp. Transport coefficients are estimated by matching upstream Thomson scattering profiles towards the start of the density ramp and remain unchanged as density increases.

Based on these modeling predictions a new V-shape geometry was installed in DIII-D by modifying the inner (inboard) row of carbon tiles of the SAS slot. At the same time the existing outer row of tiles were coated with a thin layer of tungsten. Details of the divertor design and the resultant change in divertor geometry are shown in Fig. 1. The expected flow patterns for the V-shape when the outer strike point is placed at the vertex are shown in Fig. 2, where for both drift directions we would expect improved density buildup near the vertex and hence improved dissipation compared to the original SAS, which allowed for significantly more flow out of the divertor in the private flux region due to its more open, flat-targeted design.

As in the original SAS research, measurements of energy dissipation were conducted for the new geometry by studying the target electron temperature T_e (measured by an array of single Langmuir probes near the strike point) using deuterium fuel density ramping to detachment. The SAS plasma shapes and parameters were duplicated for these studies. Measurements of neutral (molecular + atomic) deuterium pressures inside the slot are made using two separate ASDEX gauges, one near the vertex and one farther down the slot on the outer tile row. Fueling and/or impurity injection may be done inside the divertor slot, or in the main chamber. In the experiments, density feedback control was employed using real-time line-averaged density measurements. Experimentally, the density dependence can be characterized in terms of either the line-averaged density $< ne >$, determined from interferometry, or the upstream separatrix density n_{eSEP}. For direct comparison to the modeling results a value for ne_{SEP} is required. However, many earlier experimental studies (including on DIII-D) have relied on a 'surrogate' ne_{SEP} value based on some scaled fraction of the line-averaged density for convenience. In this study, the experimental upstream separatrix density was determined from Thomson scattering measurements and power balance determination of the separatrix location assuming flux-limited Spitzer conductivity[14]. Additional experimental details are covered in Ref [18].

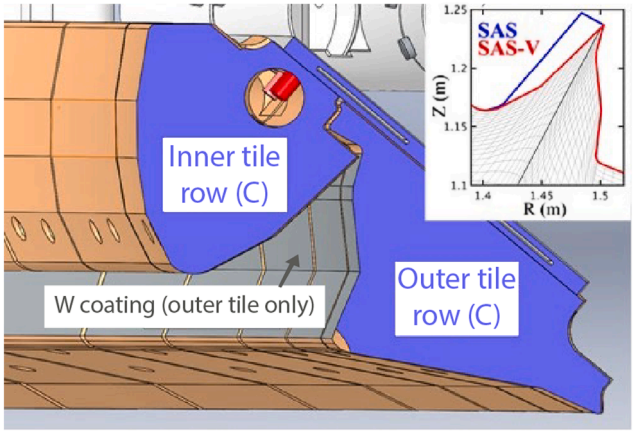

Fig. 1. Cartoon of the DIII-D SAS-VW divertor design showing the graphite inner and outer tile rows, and W-coated area. Inset: Poloidal cross section indicating the difference in limiter geometry between the SAS and SAS-VW.

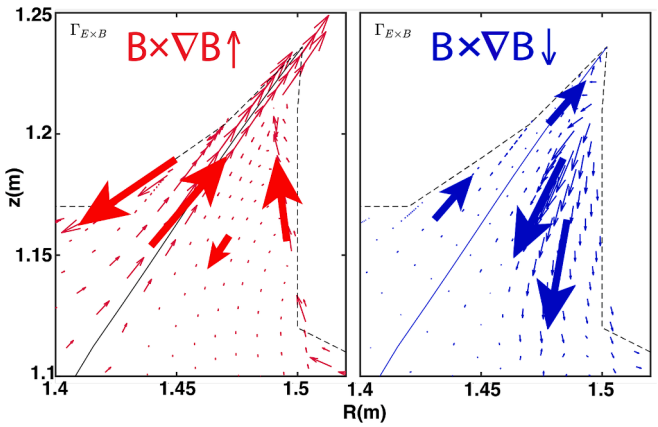

Fig. 2. **E** × **B** particle flux pattern for the two B_T directions in the SAS-VW divertor from SOLPS-ITER modeling with strike-point at the vertex. Left: With ion **B**×∇B into the divertor (up), the **E** × **B** drift moves particles from the common flux region to the private flux region. Right: with ion **B**×∇B out of the divertor (down), the **E** × **B** drift moves particles from the inner divertor to the outer private flux region and to the outer common flux region.

Results on SAS-VW

Comparing the experimental results with the most recent drift-dependent modeling for the new geometry [13], we find fairly good agreement at early points in the dissipation/detachment process where T_e is still above ~ 10 eV. (Fig. 3). The divergence between modeling and experiment at higher n_{eSEP} and lower target T_e is partially due to reduced Langmuir probe accuracy at the lowest T_e (below 2–3 eV for these cases). Probably more important are inaccurate modeling assumptions. For the density scan modeling shown here, the exact slope and rapid drop of the modeled T_e from [13] is influenced by the choice of static transport coefficients for the density scans. A good fit to the measured densities and temperatures was used to infer transport parameters for the point around 20 eV (n_{eSEP} ~ 1.21 x 10e19 m-3) and the same values were used for the other density points. This may be skewing the modeled results at both ends of the density scan. Additionally, limitations on gridding in the model do not allow for an exact match to the as-built slot. The effect of the tungsten coating on the outer side of the SAS-VW divertor is believed to be modest because of the strikepoint location on the graphite surfaces only, redeposited carbon covers the majority of the tungsten surface with little bare tungsten. Subsequent modeling where the carbon sputtering was varied along the outer surface resulted in a slight increase in target temperature but did not significantly affect the modeling results for these strikepoint locations.

Qualitative agreement with SAS-VW modeling was also found for experiments varying the strike point location within the slot, the location of gas puffing, and the use of low- and medium-z impurity gases to enhance energy dissipation. Fig. 4 shows the effect of in-slot gas fueling for the ion B×∇B drift into the slot case (Fig. 5A shows the fueling locations). We found that plasma detachment onset occurs at lower line-averaged plasma density with in-slot gas fueling compared to main chamber fueling, with a ~ 22 % reduction for strike point on the vertex and a ~ 7 % reduction for strike point on the (HFS) inner slant. This is a consequence of the in-slot puffing in this closed geometry having better fuel retention, leading to a higher separatrix density in the divertor and hence better dissipation for a given line-averaged density, as can be seen from the parametric plot of n_{eSEP} vs $< ne >$ on the right. It is evident from this plot that the requirement for adequate dissipation in SAS-VW is a certain level of n_{eSEP} (~2–3 x 10^{19} m^{-3}) and not the specific main chamber density. The rapid increase in n_{eSEP} with $< n_e >$ also points out the error of using a fixed fraction of $< ne >$ as the independent variable when studying dissipation in divertors. The in-slot fueling effect is consistent with results seen in earlier SAS experiments [15]. The effect persists but is less pronounced (~5%) with ion B×∇B drift out of slot. The retention effect is captured by SOLPS-ITER simulations, showing a ~ 20 % reduction of the upstream separatrix density required to lower the target temperature to ~ 10 eV near the strike point with in-slot compared to main-chamber fueling.

In-slot N_2 (25 TorrL/s) further lowered the upstream separatrix density required to reach detachment by ~ 14 % compared to in-slot D_2 puffing. Compared to main chamber puffing, in-slot N_2 puffing also led to less confinement degradation and lower core Zeff after detachment, presumably due to the efficient retention of impurities in the SAS-VW geometry (Fig. 5).

Locating the outer strike point on the inner slant (inboard) side of SAS-VW results in earlier detachment onset than for the strike point located at vertex. Similar experimental results were seen for the strike point located on the inner surface of the original SAS [16], although in SAS-VW these results are obtained for both drift directions, and agree with modeling. SOLPS-ITER indicates the poloidal E × B flux can be up to 10X higher in the ion B×∇B drift out of the divertor case for SAS-VW versus SAS, enhancing particle flow to the near-SOL and leading to better dissipation and a double-peaked T_e profile along the target [17].

Discrepancies with modeling

In contrast to the modeling predictions that the drift-dependent asymmetry in dissipation would be decreased by ~ 10 % in the new geometry [18], this was not the case experimentally (Fig. 6), where the preference for detachment in the non-favorable ion B × ∇B drift

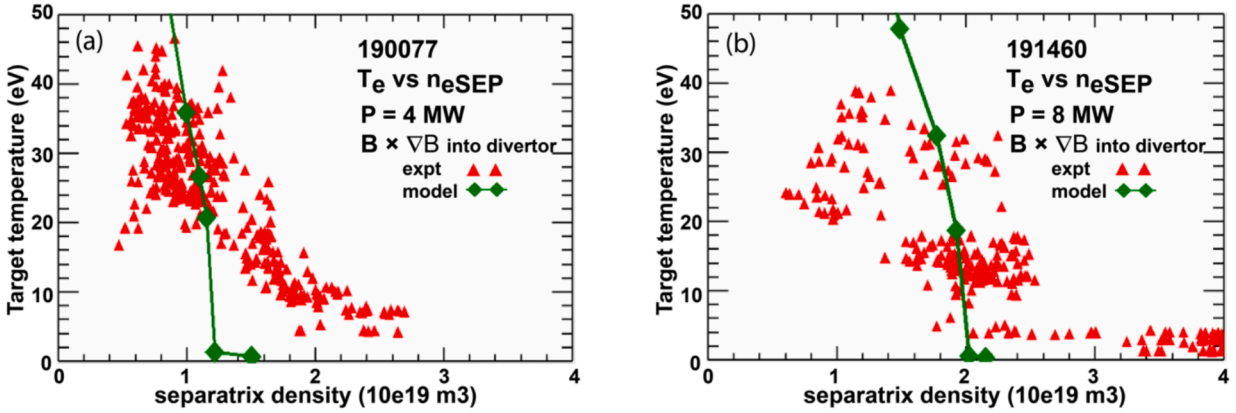

Fig. 3. Comparison of drift-dependent modeling [Ref. 13, green curves] of SAS-VW for the ion **B** × ∇B drift into the divertor. Shown is the target temperature in the near SOL ($\Psi_N = 1.007$) determined from Langmuir probes as the upstream separatrix density is increased through main-chamber D_2 puffing. Agreement is good in the Te > 10 eV range when upstream separatrix density is used. (a): shot 190,077 (P_{INJ} = 4 MW); (b): shot 191,460 (P_{INJ} = 8 MW).

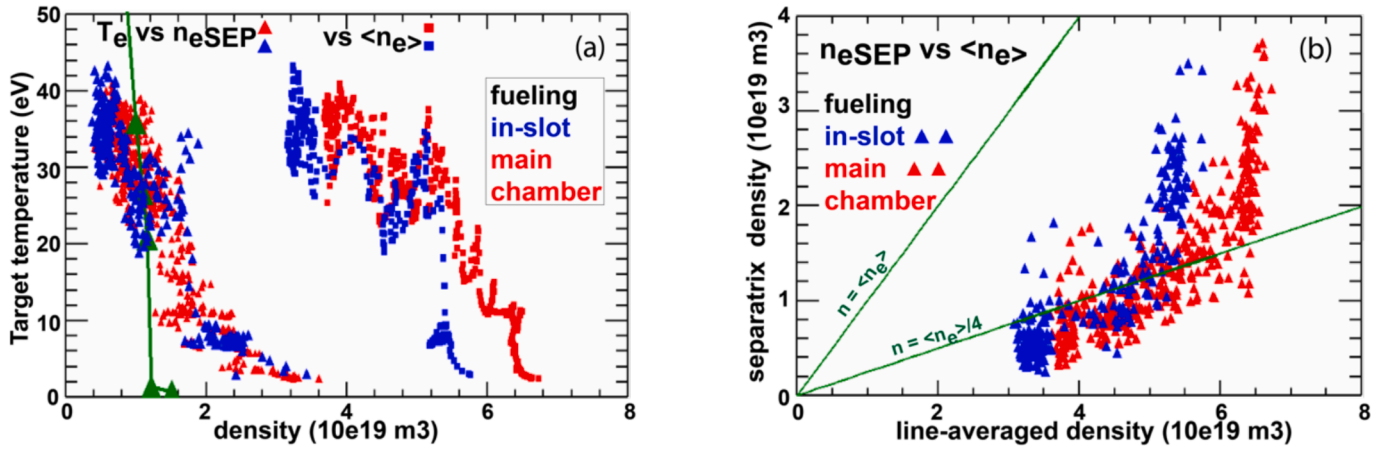

Fig. 4. (a) Effect of main-chamber (red) and in-slot (blue) puffing on target T_e as function of separatrix density (triangles) and line-averaged-density (squares) for the same data as show in Fig. 3a. (b) parametric plot of n_{eSEP} versus line-averaged density for the two cases. Green lines indicate 1.0 and 0.25 linear scalings for density. In slot puffing results in better retention in the divertor and better dissipation (higher n_{eSEP}) for a given upstream < ne > .

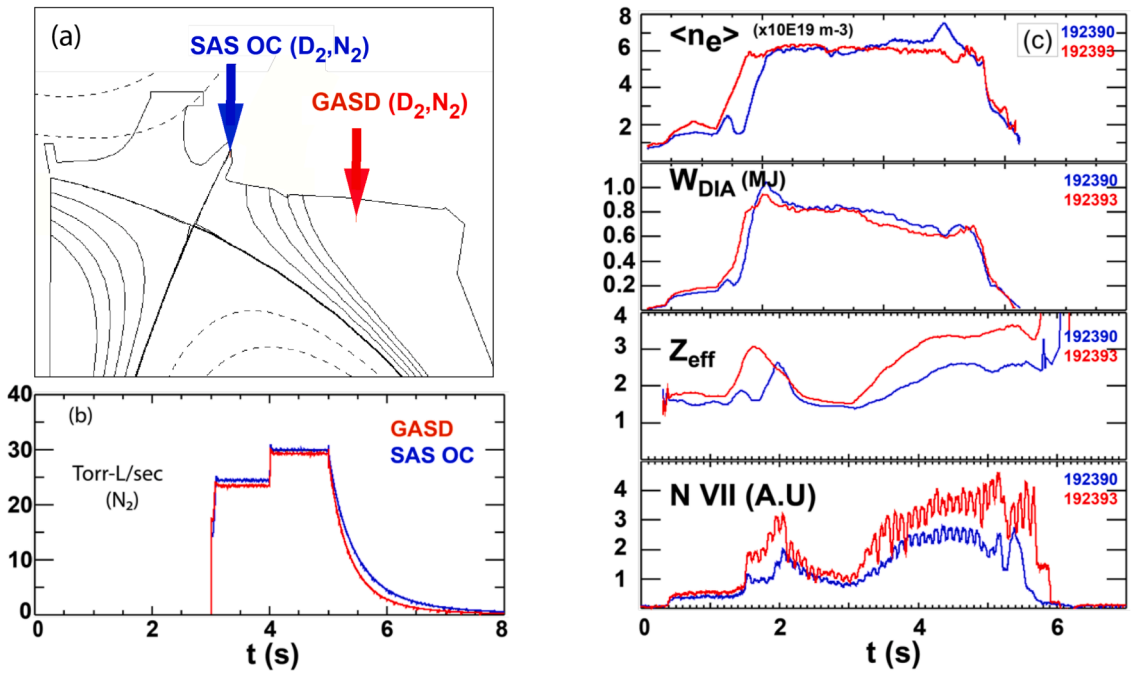

Fig. 5. Results of nitrogen seeding for main chamber (red) and in slot (blue) puffing. (a) deuterium and nitrogen injection locations for in-slot and main chamber fueling (b) N_2 injection levels for comparison shots (c) time traces of density, stored energy, z_{eff} and core nitrogen levels demonstrating higher confinement and lower core contamination after detachment with in slot injection.

direction (out of the divertor) persists. Here we also plot Te versus the line-averaged main chamber plasma density, which shows a cliff-like feature for the detachment for the ion B × ∇B drift in direction. This feature occurs at the point when sufficient density buildup occurs in the divertor for the target temperature to drop below 10 eV, where ionization and ion-neutral interactions become predominant.

Additional experiment/modeling discrepancies are seen when comparing matched discharges between the new and old geometries (Fig. 7). Experimentally, detachment onset occurs at about the same upstream separatrix density in the SAS-VW divertor as for SAS, in contrast to the SOLPS-ITER modeling predictions. This is true for both B_T directions.

Similar detachment dynamics occur for SAS-VW despite achieving significantly higher neutral pressures and compression (Fig. 8) than in the earlier geometry. Using ASDEX gauge data to infer neutral pressures near the strike point (inlet close to the LP location near the vertex) and in the far SOL (inlet farther down the slot), we find the following. For the ion $\mathbf{B}\times\nabla B$ drift into the slot (reversed B_T), the SAS-VW pressure is 3.4X higher prior to detachment and the compression 2.6X higher, compared to the original SAS. For the ion $\mathbf{B}\times\nabla B$ drift out of the slot case (forward B_T), the SAS-VW pressure is 5X higher than SAS prior to detachment (i.e, twice the reversed B_T value). Compression in this case is up to 6.5X higher than SAS, but drops quickly at higher pressures as more neutrals drift to the far SOL prior to detachment.

Discussion

Based on SOLPS-ITER simulations, the expectation for improved dissipation in the new SAS-VW is based on the following sequence of events: The combination of E × B drifts plus shaping leads to increased

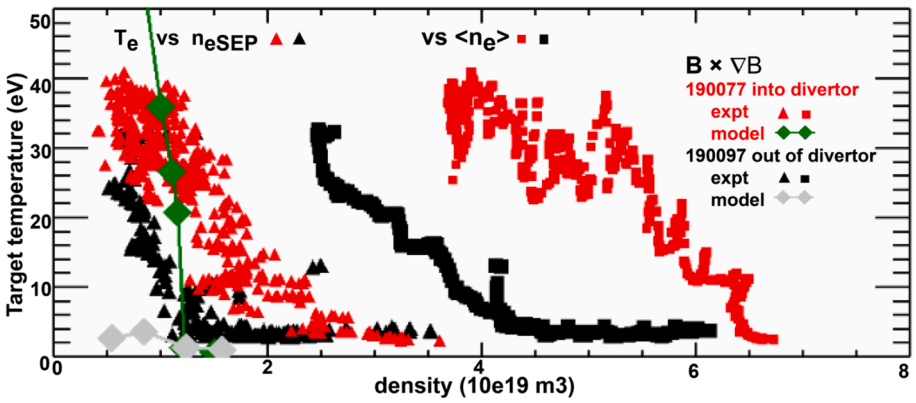

Fig. 6. Plot of SAS-VW target temperature evolution near the strike point for shots with the ion **B** × ∇B drift into [red] or out of [black] the divertor for a density ramp using main chamber deuterium puffing. Strike point was held steady at the vertex. The data are plotted versus line-averaged density (squares) as well as the separatrix density estimated from power balance calculations (triangles). Note the rapid drop into detachment at ~<ne > 6.5 x 10^{19} m^{-3} for the ∇B drift into case essentially disappears when the latter density parameter is used. Modeling results from Ref 13 are shown for both ion **B** × ∇B drift into [green] or out of [gray] directions.

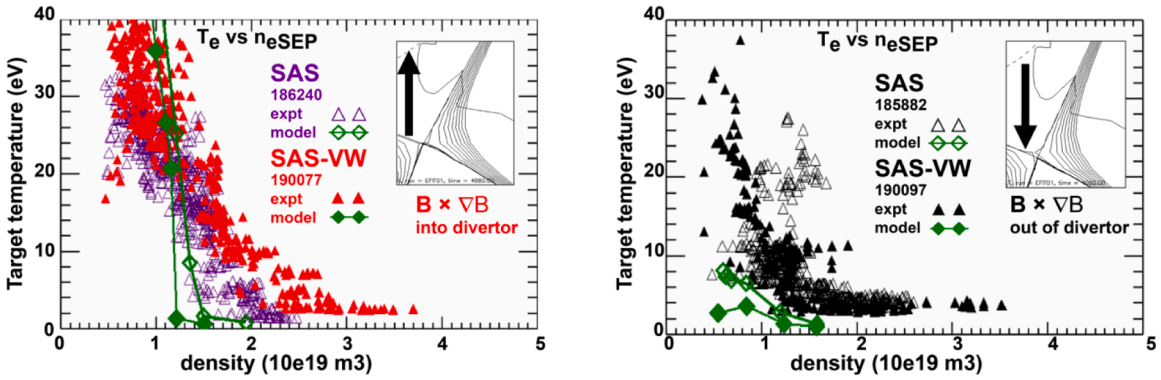

Fig. 7. Energy dissipation and detachment onset for matched 1 MA, 4 MW shots for the original SAS (open triangles) and SAS-VW (closed triangles) for both ion **B** × ∇B drift directions. Essentially the same separatrix density is required for both geometries. SOLPS-ITER modeling results [Ref 13] for both SAS (green open diamonds) and SAS-VW (green closed diamonds) are included for the two drift directions.

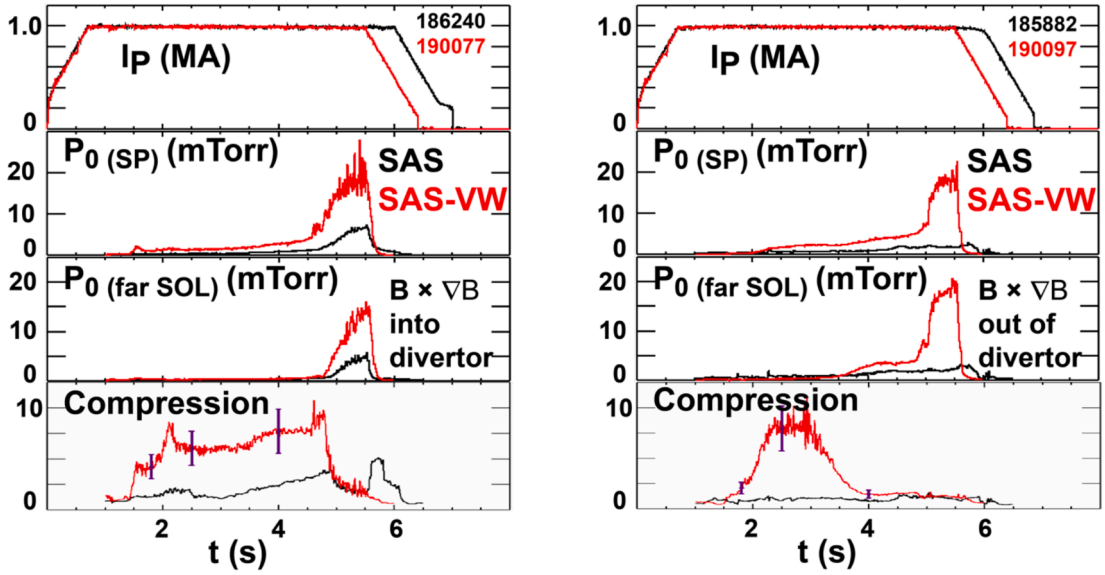

Fig. 8. Time traces of the neutral pressure measured near the outer strike point at the vertex and in the far SOL for SAS-VW (red) and original SAS (black) matched shots, for both drift directions. Also plotted is the ratio of the two neutral pressures as an indication of neutral compression in the slot.

neutral buildup in the slot compared to the original SAS. The increased neutral density increases the energy dissipation in the divertor, which decreases the temperature upstream of the target. This decreased temperature gradient in turn decreases the electric field, which decreases the drive for local flow patterns. This modification of the flow patterns has three beneficial effects: (1) the decreased flow in the relatively closed divertor should decrease the upstream leakage of particles, further increasing the neutral density and dissipation; (2) this decreased leakage represents a better decoupling of the divertor from the main plasma which manifests in lower upstream densities for detachment; and (3) the lessened flow into the private flux region should decrease the asymmetry in detachment behavior for the two drift directions. All of these effects should enhance the energy dissipation performance relative to the original SAS shape.

In the experiment we only observe part of this sequence. As seen in Fig. 8, the new divertor shape is effective at increasing neutral density buildup for both drift directions compared to the original SAS. However, despite significantly higher neutral pressure and compression we find similar detachment dynamics for SAS and SAS-VW, resulting in similar upstream separatrix densities at detachment. One possibility is that the estimated neutral densities required for dissipation from modeling are too high, or that the dissipation is occurring in regions where the neutral measurements are not made. Integration of the existing pressure measurements as a synthetic diagnostic might help understand this discrepancy, as might the more complex process of incorporating the neutral measurements as a direct constraint on the modeling. Another open question is the accurate modeling of the expected decrease in shaping efficiency as opacity increases at higher plasma densities and collisionalities [13] and it might be that the experiment is in this region. This may also partially explain why the drift asymmetry in dissipation remains for the new shape, although slightly diminished. Another possible complication in comparing the two geometries is the existence of tungsten in the outer part of the newer divertor, although for the experiments described here the strikepoint is on graphite and the metal surface should be predominantly covered with carbon.

While there are a number of improvements that can be made in the modeling (incorporating more realistic transport parameters, better meshing at the fine scales required for these relatively small geometries, addressing long convergence times by migrating to newer and faster systems) and the experiment (better signal-to-noise for Thomson density measurements in the slot, improved viewing access of the slot for flow visualization and other diagnostics), the present lack of fidelity between well-converged code runs and a relatively well-diagnosed divertor experiment is concerning. SOLPS-ITER is one of the primary design tools for future divertors, on machines which will be far more demanding in terms of their power handling requirements and the relative difficulty of implementing comprehensive diagnostics.

Future work will involve further variation of parameters in the code runs, as well as further post-processing of the existing run results to try and pin down whether the simulations are being done with adequate sensitivity and precision, or whether there is missing physics in these simulations. In addition, the DIII-D program plans a series of near term divertor upgrades to facilitate performance at higher triangularity and plasma volume, negative triangularity, and optimized particle and heat control for optimized core–edge integration. Each of these upgrades will provide us with additional opportunities in different parameter ranges for continued code validation and improvements.

CRediT authorship contribution statement

D.M. Thomas: Writing – review & editing, Writing – original draft, Visualization, Validation, Supervision, Software, Project administration, Methodology, Investigation, Formal analysis, Data curation, Conceptualization. **T. Abrams:** Validation, Investigation, Formal analysis, Conceptualization. **R. Ding:** Writing – original draft, Visualization, Methodology, Investigation, Formal analysis, Data curation, Conceptualization. **D. Donovan:** Software, Resources, Methodology, Data curation. **F. Effenberg:** Writing – original draft, Resources, Methodology, Investigation, Formal analysis, Data curation, Conceptualization. **J. Herfindal:** Software, Resources, Methodology, Formal analysis, Data curation. **A. Hyatt:** Software, Resources, Methodology, Investigation, Formal analysis, Data curation. **A.W. Leonard:** Writing – review & editing, Validation, Methodology, Formal analysis, Conceptualization. **X. Ma:** Writing – original draft, Visualization, Validation, Software, Methodology, Investigation, Formal analysis, Data curation, Conceptualization. **R. Maurizio:** Writing – review & editing, Writing – original draft, Visualization, Validation, Software, Methodology, Investigation, Formal analysis, Data curation, Conceptualization. **A.G. McLean:** Writing – review & editing, Methodology, Investigation, Data curation, Conceptualization. **C. Murphy:** Resources, Methodology, Data curation, Conceptualization. **J. Ren:** Writing – original draft, Visualization, Validation, Software, Resources, Methodology, Investigation, Formal analysis, Data curation, Conceptualization. **M.W. Shafer:** Writing – review & editing, Software, Resources, Formal analysis, Data curation, Conceptualization. **D. Truong:** Software, Resources, Methodology, Investigation, Formal analysis, Data curation. **H.Q. Wang:** Writing – review & editing, Writing – original draft, Visualization, Validation, Software, Resources, Methodology, Investigation, Formal analysis, Data curation, Conceptualization. **J.G. Watkins:** Visualization, Software, Resources, Methodology, Formal analysis, Data curation, Conceptualization. **J.H. Yu:** Writing – original draft, Writing – review & editing, Software, Visualization, Validation, Resources, Methodology, Investigation, Formal analysis, Data curation, Conceptualization.

Declaration of competing interest

The authors declare that they have no known competing financial interests or personal relationships that could have appeared to influence the work reported in this paper.

Acknowledgements

This material is based upon work supported by the U.S. Department of Energy, Office of Science, Office of Fusion Energy Sciences, using the DIII-D National Fusion Facility, a DOE Office of Science user facility, under Awards DE-FC02-04ER54698, DE-NA0003525, DE-AC52-07NA27344, DE-AC05-00OR22725, DE-SC0023378.

Data availability

Data will be made available on request.

References

[1] P.C. Stangeby, A.W. Leonard, Obtaining reactor-relevant divertor conditions in tokamaks, Nucl Fusion 51 (2011) 063001.
[2] P.C. Stangeby, Basic physical processes and reduced models for plasma detachment Plasma Phys, Control. Fusion 60 (2018) 044022.
[3] J.A. Boedo, M.J. Schaffer, R. Maingi, C.J. Lasnier, Electric field-induced plasma convection in tokamak divertors, Phys. Plasmas 7 (2000) 1075.
[4] X. Bonnin, W. Dekeyser, R. Pitts, D. Coster, S. Voskoboynikov, S. Wiesen, Presentation of the New SOLPS-ITER Code Package for Tokamak Plasma Edge Modelling Plasma Fusion Res. 11 (1) (2016) 403102.
[5] R. Schneider, X. Bonnin, K. Borrass, D.P. Coster, H. Kastelewicz, D. Reiter, V. A. Rozhansky, B.J. Braams, Plasma edge physics with B2-eirene Contrib, Plasma Phys. 46 (2006).
[6] D. Reiter, M. Baelmans, P. Börner, The eirene and B2- eirene codes Fusion Sci, Technol. 47 (2005) 172–186.
[7] H.Y. Guo, C.F. Sang, P.C. Stangeby, L.L. Lao, T.S. Taylor, D.M. Thomas, Small angle slot divertor concept for long pulse advanced tokamaks, Nucl. Fusion 57 (2017) 044001.
[8] C. Sang, H.Y. Guo, P.C. Stangeby, L.L. Lao, T.S. Taylor, SOLPS analysis of neutral baffling for the design of a new diverter in DIII-D, Nucl. Fusion 57 (2017) 056043.
[9] P.C. Stangeby, C. Sang, Strong correlation between D2 density and electron temperature at the target of divertors found in SOLPS analysis, Nucl. Fusion 57 (2017) 056007.

[10] H.Y. Guo, et al., First experimental tests of a new small angle slot divertor on DIII-D, Nucl. Fusion 57 (2019) 086054.
[11] X. Ma, H.Q. Wang, H.Y. Guo, P.C. Stangeby, E.T. Meier, M.W. Shafer, D. M. Thomas, First evidence of dominant influence of E × B drifts on plasma cooling in an advanced slot divertor for tokamak power exhaust, Nucl. Fusion 61 (2021) 054002.
[12] H. Du, H.Y. Guo, P.C. Stangeby, X. Bonnin, G. Zheng, X. Duan, M. Xu, Manipulation of E × B drifts in a slot divertor with advanced shaping to optimize detachment Nucl, Fusion 60 (2020) 126030.
[13] R. Maurizio, H. Du, A. Gallo, H.Y. Guo, A. Leonard, X. Ma, G. Sinclair, P. Stangeby, D.M. Thomas, H. Wang, R.S. Wilcox, J.H. Yu, L. Casali, M.W. Shafer, 2021 Numerical assessment of the new V-shape small-angle slot divertor on DIII-D Nucl, Fusion 61 (2021) 116042.
[14] A.W. Leonard, A. McLean, M.A. Makowski, P.C. Stangeby, Compatibility of separatrix density scaling for divertor detachment with H-mode pedestal operation in DIII-D 2017 Nucl, Fusion 57 (2017) 086033.
[15] H.Q. Wang, X. Ma, R. Maurizio, H.Y. Guo, D.M. Thomas, J.G. Watkins, M. W. Shafer, A.W. Hyatt, A.L. Moser, J. Ren, A. McLean, F. Scotti, P. Stangeby, Dependence of particle and power dissipation on divertor geometry and plasma shaping in DIII-D small-angle-slot divertor, Nucl. Mater. Energy 33 (2022) 101301.
[16] M.W. Shafer, B. Covele, J.M. Canik, L. Casali, H.Y. Guo, A.W. Leonard, J.D. Lore, A. G. McLean, A.L. Moser, P.C. Stangeby, D. Taussig, H.Q. Wang, Watkins, Dependence of neutral pressure on detachment in the small angle slot divertor at DIII-D Nucl, Mater. Energy 19 (2019) 487–492.
[17] X. Ma, D.M. Thomas, R. Maurizio, A.G. McLean, J. Ren, M.W. Shafer, F. Scotti, D. Truong, H.Q. Wang, J.H. Yu, J.G. Watkins, Divertor dissipation in the DIII-D V-shaped slot divertor with strong external heating, APS-DPP (2023).
[18] R. Maurizio, D.M. Thomas, J.H. Yu, T. Abrams, A.W. Hyatt, J. Herfindal, A. Leonard, X. Ma, A.G. Mclean, J. Ren, F. Scotti, M.W. Shafer, G. Sinclair, H. Q. Wang, J. Watkins, Experiments on plasma detachment in a V-shaped slot divertor, IAEA 2023 (London), Nucl. Fusion 64 (2024) 086048.